Thermodynamic study of c-axis-oriented epitaxial Pb(Zr,Ti)O-3 thin films

AUTHOR(S):

Kanno, I; Yokoyama, Y; Kotera, H; Wasa, K

CITATION:

Kanno, I ...[et al]. Thermodynamic study of c-axis-oriented epitaxial Pb(Zr,Ti)O-3 thin films. PHYSICAL REVIEW B 2004, 69(6): 064103.

ISSUE DATE:

2004-02

URL:

http://hdl.handle.net/2433/50138

PHYSICAL REVIEW B **69**, 064103 (2004)

Thermodynamic study of *c*-axis-oriented epitaxial $Pb(Zr,Ti)O_3$ thin films

Isaku Kanno, Yu Yokoyama, and Hidetoshi Kotera
Department of Mechanical Engineering, Kyoto University, Yoshida-honmachi, Sakyo-ku, Kyoto 606-8501, Japan

Kiyotaka Wasa
Faculty of Science, Yokohama City University, Yokohama 236-0027, Japan

(Received 1 August 2003; revised manuscript received 2 October 2003; published 12 February 2004)

Thermodynamic characteristics of single crystalline $Pb(Zr_{0.52}Ti_{0.48})O_3$ (PZT) were investigated using *c*-axis oriented PZT films. The PZT films were epitaxially grown on Pt/MgO substrate and dielectric and ferroelectric properties were measured as a function of one-dimensional stress. The stress dependence of dielectric and ferroelectric properties was examined on the basis of the Landau-Devonshire's phenomenological theory and the free energy coefficients of single crystalline PZT films were obtained. The dielectric stiffness coefficients and electrostrictive coefficient of epitaxial PZT films were obtained to be $\alpha_1 = -1.30\times10^8$ (m/F), $\alpha_{11} = 3.07\times10^8$ (m^5/C^2F), $\alpha_{111} = -3.11\times10^7$ (m^9/C^2F), and $Q_{12} = -5.70\times10^{-2}$ (m^4/C^2), which are different from the values derived from the analysis of polycrystalline PZT. The temperature dependence of dielectric constant of the PZT films showed clear Curie-Weiss law and the dielectric stiffness coefficient α_1 derived from this measurement was almost same value from the analysis of stress dependence of the dielectricity of the epitaxial PZT films.

DOI: 10.1103/PhysRevB.69.064103 PACS number(s): 77.55.+f, 77.84.Dy, 77.80.Bh

I. INTRODUCTION

The $Pb(Zr,Ti)O_3$ (PZT) ferroelectric materials have attracted considerable attention due to their excellent dielectric, ferroelectric, and piezoelectric properties. Ferroelectric properties of PZT can be theoretically analyzed by thermodynamic formalism on the basis of the Landau-Devonshire phenomenological theory and lots of investigations have been reported concerning electrical properties and crystalline phases of $PbTiO_3$-$PbZrO_3$ solid solution system.[1–3] Haun *et al.* investigated PZT with a variety of Zr/Ti ratio based on the Landau-Devonshire formula in detail and derived free energy coefficients in this system.[4–6] These thermodynamic coefficients of PZT have been used as the standard values to investigate thermodynamic studies of PZT in later research. In recent years, the development of the ferroelectric thin films has been significantly progressed as promising materials for use in nonvolatile memories and in microelectromechanical systems (MEMS).[7–9] The characterization of the ferroelectric PZT thin films have been performed on the basis of the thermodynamic phenomenological theory using conventional free energy coefficients derived from the analysis of bulk PZT.[10–13] Oh *et al.* have already carried out the detailed analysis of the effects of two-dimensional stress on the epitaxial PZT thin films and revealed the relationship between stress and phase diagram on the basis of thermodynamic theory.[14] The thermodynamic equations can be expressed by spontaneous polarization and stress of single crystalline PZT. However, since it has been impossible to grow PZT single crystal with enough size for measurements of electric properties, conventional values of free energy function were derived from indirect method using polycrystalline PZT ceramics.

On the other hand, thin film deposition techniques such as rf sputtering and chemical vapor deposition enable an epitaxial growth of PZT films with single crystalline structure.[15–19] In comparison with polycrystalline PZT ceramics, single crystalline epitaxial films exhibit several unique characteristics such as anomalous crystalline structure due to not only extrinsic stress from the substrate but intrinsic stress due to impinging energetic species onto the films.[18–20] Therefore it is necessary to perform thermodynamic analysis and derive free energy coefficients using the epitaxial PZT films instead of the conventional bulk values. Fortunately, the crystalline structure of tetragonal PZT films with *c*-axis orientation is so simple that it is relatively easy to evaluate stress effects on the electric properties. In this study, we prepared *c*-axis oriented epitaxial PZT films with the composition near morphotoropic phase boundary and measured the dielectric and ferroelectric properties as a function of one-dimensional stress along the *a* or *b* axis of the tetragonal unit cell. Several coefficients of free energy function of epitaxial PZT films were experimentally derived and compared with conventional values of bulk PZT derived by Haun *et al.*[5] In addition, we have estimated the dielectric and ferroelectric characteristics of epitaxial PZT films under a wide range of external stress using free energy coefficients we derived through this study.

II. EXPERIMENTS

A. Preparation of PZT thin films

PZT thin films were deposited using rf magnetron sputtering. Pt electrodes with the thickness of 100 nm were epitaxially grown on (100)MgO substrates prior to PZT growth. The sputtering conditions of PZT films were described in previous reports.[18,19] The target used was hot-pressed ceramics of which composition was near morphotoropic phase boundary of Zr/Ti=53/47 including additional PbO for the compensation of reevaporation of lead. The growth of the PZT was carried out at the substrate temperature of 550 °C. The thickness of the PZT films we prepared was 3 μm from

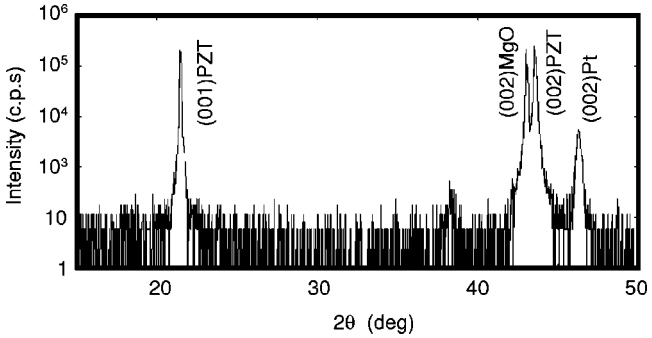

FIG. 1. XRD pattern of the PZT film grown on a (100)Pt/(100)MgO substrate. The PZT film was perfectly oriented along the *c* axis.

the viewpoint of MEMS applications. In addition, the thin films as thick as 3 μm is desirable to eliminate the thickness dependence of the PZT films.[21] The composition of the resulting films was evaluated by energy dispersive x-ray spectroscopy and was identified as Zr/Ti=52/48 that was almost same ratio of target one. Figure 1 shows x-ray diffraction (XRD) pattern of the PZT thin films. Strong peaks of (001) and (002)PZT can be observed without any other phases. We have also analyzed crystalline structure using four-circle XRD and reciprocal space maps of (004) and (204)PZT were shown in Fig. 2. In the reciprocal space map of (004)PZT diffraction [Fig. 2(a)], we could observe only single peak of the PZT and there were no peaks corresponding to 90° domains which appear near the side of (004)PZT diffraction. Furthermore, in the reciprocal map of (204) diffraction [Fig. 2(b)], the peak position of (204)PZT is located at the right side from the dotted line passing through (204)MgO and (204)Pt. This result indicates $a<c$, that the PZT films have tetragonal structure. From the peak positions of (004) and (204)PZT, the lattice constants of *a* and *c* were calculated as 4.049 and 4.161 Å, respectively.

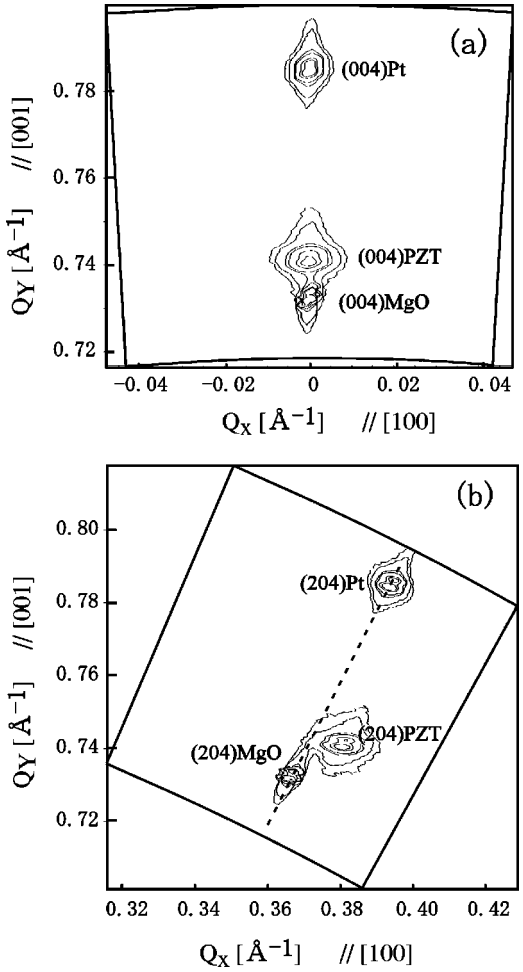

FIG. 2. Reciprocal space maps of the PZT films on (100)Pt/(100)MgO covering the reflections of (a) (004)PZT and (b) (204)PZT. A dotted line is drawn as passing through (204)MgO and (204)Pt.

B. Measurement of residual stress

Epitaxial films generally have significant residual stress due to lattice mismatch as well as difference of thermal expansion coefficients between films and substrates. Particularly, PZT films were deposited at high substrate temperatures of 550 °C which induced large thermal stress during cooling down to a room temperature. In order to identify influence of internal stress on electric properties, we have to evaluate the residual stress accumulated in the PZT films prior to the evaluation of the stress effects on the electric properties. For the measurement of the residual stress, we cleaved PZT/Pt/MgO samples into strip specimens and evaluated one-dimensional residual stress of epitaxial PZT films along the length of the specimen. The specimen was cut as the directions of length and width are along *a* and *b* axes. The dimension of the specimen was listed in Table I. The width of the specimen is smaller than the length. Therefore the stress of the width direction is relaxed compared with the stress along the length and we can neglect the influence of the stress of the width direction. The curvature of the specimen was measured by surface profiler. In order to obtain adequate bending of the specimen, the thickness of the MgO substrate was reduce by wet etching from 0.3 to 0.19 mm prior to the measurement of the curvature.

Then the electric properties of the PZT films were evaluated as a function of external stress using the cantilever specimen similar with the specimen for curvature measurements. The one end of the specimen was fixed by a vise as illustrated in Fig. 3, and then one-dimensional stress was

TABLE I. Dimension of the specimen for residual stress measurement.

	MgO	PZT
Thickness h (m)	0.19×10^{3}	3.0×10^{-6}
Width of the specimen b (m)	3.03×10^{-3}	
Young's modulus E (Pa)	248×10^{9}	92.6×10^{9}
Thermal expansion coefficient α_T (°C)	13.8×10^{-6}	
Temperature difference ΔT (°C)	525	

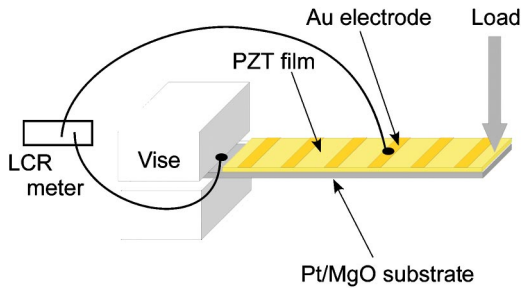

FIG. 3. Illustration of the measurement system of the electric properties with application of one-dimensional stress over the PZT films.

imposed on the PZT films along the length of the cantilever by putting the load at the other end of cantilever. In the case of the application of compressive stress on the PZT films, the load was put on the PZT film, while in the case of the tensile stress the specimen was upside down and the load was applied on the MgO substrate. In this experiment, the maximum load we used was 50 gf. Stripe-shaped electrodes with the width of 1 mm were deposited on the PZT films and the external stress at the electrode can be determined by the load and the distance from the load point. The dielectric constants and *P-E* hysteresis loops were measured as a function of induced one-dimensional stress in the PZT films.

III. RESULTS AND DISCUSSION

A. Evaluation of residual stress

The residual stress was evaluated by means of measuring the bending of the substrate. In this measurement, we calculated the radius of curvature R of the PZT/MgO (thickness of 0.19 mm). The bending of the beam was 2.15 μm at a distance of 2.5 mm along the length and the radius of curvature R was calculated to be 1.45 m in this specimen. The stress on PZT films σ is expressed as

$$\sigma = -\frac{2(E_1 I_1 + E_2 I_2)}{R(h_1+h_2)bh_2}, \tag{1}$$

where E, I, h, b are the Young's modulus, the moment of inertia, the thickness, and the width. The subscript 1 and 2 denote MgO substrate and PZT film. We neglect the effects of the Pt electrode due to its small thickness compared with that of MgO and PZT. The Young's modulus of single crystal MgO is reported as 248 GPa,[22] while the Young's modulus of epitaxial PZT films was 92.6 GPa which we measured and reported in a previous paper.[23] From Eq. (1), σ becomes -338 MPa of compressive stress.

On the other hand, assuming the stress of the PZT films was caused by the difference of the thermal expansion coefficients with MgO substrate, the strain at the interface of PZT/MgO was written by

$$\frac{h_1/2}{R} - \frac{\sigma h_2}{E_1 h_1} - \alpha_{T1}\Delta T = -\frac{h_2/2}{R} + \frac{\sigma}{E_2} - \alpha_{T2}\Delta T, \tag{2}$$

where α_{T1} and α_{T2} are the thermal expansion coefficients of MgO and PZT films, and ΔT is the difference between a deposition temperature and a room temperature. The thermal expansion coefficient of single crystal MgO is reported to be $\alpha_{T1} = 13.8\times10^{-6}$ (°C),[24] therefore that of the epitaxial PZT was calculated to be $\alpha_{T2} = 6.69\times10^{-6}$ (°C). On the other hand, the radius of curvature R_0 of the PZT films on 0.3-mm-thick MgO was given from the Eq. (1) and (2)

$$\frac{1}{R_0} = \frac{(\alpha_{T1}-\alpha_{T2})T}{(h_1+h_2)/2 + 2(E_1h_1+E_2h_2)(E_1I_1+E_2I_2)/[E_1h_1E_2h_2b(h_1+h_2)]}. \tag{3}$$

From Eqs. (1) and (3), the residual stress of the as-grown PZT films on the MgO substrate with a thickness of 0.3 mm was determined as $\sigma_0 = -340$ MPa of compressive stress. The residual stress only affects the *a* axis (or *b* axis) since the PZT films are epitaxially grown with the perfect *c*-axis orientation on the MgO substrates and the specimen is cleaved out along the *a* or *b* axis.

B. Stress dependence of electric properties

The relative dielectric constants of the PZT films were measured as a function of extrinsic one-dimensional stress. The extrinsic stress σ^* from the load to the PZT was given as

$$\sigma^* = E_2\frac{My}{E_1I_1+E_2I_2}, \tag{4}$$

where M and y are the moment and the distance from the neutral axis of the specimen. Figure 4 shows the relative dielectric constants of the PZT films as a function of the one-dimensional stress. Since the PZT films suffer large compressive stress σ_0 of -340 MPa, the total stress on the PZT films $\sigma = \sigma^* + \sigma_0$ was within the compressive region. The measurements revealed that the relative dielectric constants of the *c*-axis-oriented epitaxial PZT films increased as the compressive stress was reduced.

In addition, *P-E* hysteresis loops were also observed applying the different internal stress for PZT films. Figure 5 shows the *P-E* hysteresis loops of the PZT films with different one-dimensional stresses. The PZT films suffered additional compressive and tensile stress of 50 MPa from the as-grown state and the loops were slightly changed by the external stress. The remanent polarization (P_r) was plotted in Fig. 6 as a function of the internal stress of the PZT films.

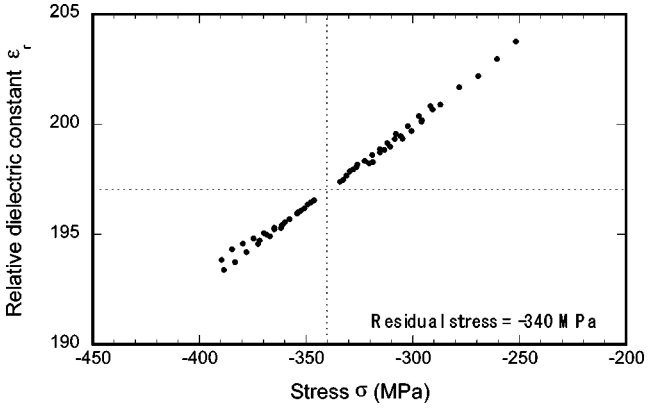

FIG. 4. Relative dielectric constant of the *c*-axis-oriented PZT films as a function of the one-dimensional stress along the *a* axis. The stress σ is given by the sum of the residual stress σ_0 and external stress σ'.

Although the obtained values were relatively scattered, we observed clear stress dependence as the remanent polarization increased with applying compressive stress, while it decreased with applying tensile stress.

C. Thermodynamic analysis

The Gibbs free energy function for PZT is expressed as

$$\begin{aligned}\Delta G = {} & \alpha_1(P_1^2+P_2^2+P_3^2)+\alpha_{11}(P_1^4+P_2^4+P_3^4)+\alpha_{12}(P_1^2P_2^2 \\ & +P_2^2P_3^2+P_3^2P_2^2)+\alpha_{111}(P_1^6+P_2^6+P_3^6)+\alpha_{112}\{P_1^4(P_2^2 \\ & +P_3^2)+P_2^4(P_3^2+P_1^2)+P_3^4(P_1^2+P_2^2)\}+\alpha_{123}P_1^2P_2^2P_3^2 \\ & -\frac{1}{2}s_{11}(X_1^2+X_2^2+X_3^2)-s_{12}(X_1X_2+X_2X_3+X_3X_1) \\ & -\frac{1}{2}s_{44}(X_4^2+X_5^2+X_6^2)-Q_{11}(X_1P_1^2+X_2P_2^2+x_3P_3^2) \\ & -Q_{12}\{X_1(P_2^2+P_3^2)+X_2(P_3^2+P_1^2)+X_3(P_1^2+P_2^2)\} \\ & -Q_{44}(X_4P_2P_3+X_5P_3P_1+X_6P_1P_2), \end{aligned} \quad (5)$$

where P_i and X_i are the polarization and stress; α_i, α_{ij}, and α_{ijk} are the dielectric stiffness coefficients at constant stress; s_{ij} are the elastic compliances at constant polarization; and Q_{ij} are the electrostrictive constants. In the reduced notation, the tensile stresses are denoted by X_1, X_2, X_3 and shear stressed by X_4, X_5, X_6.

Since the PZT films we prepared showed tetragonal structure, the following conditions should be satisfied in Eq. (5): $P_1=P_2=0$, $P_3\neq 0$. In the experiments we applied one-dimensional stress along the length of the beam-shaped specimen, and we can define the following conditions of the stress: $X_1=\sigma$, $X_2=X_3=X_4=X_5=X_6=0$. Therefore, Eq. (5) in the epitaxial PZT films with tetragonal phase results in the equations

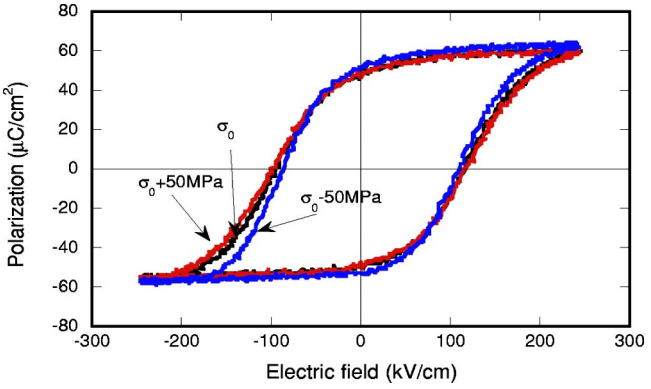

FIG. 5. *P-E* hysteresis loops of the PZT films with different external one-dimensional stress of −50, 0, and +50 MPa.

$$\Delta G = \alpha_1 P_3^2+\alpha_{11}P_3^4+\alpha_{111}P_3^6-\frac{1}{2}s_{11}\sigma^2-Q_{12}\sigma P_3^2. \quad (6)$$

Using the free energy equation, the spontaneous polarization P_3 can be derived from the condition

$$\frac{\partial \Delta G}{\partial P_3}=0,$$

$$P_3=\sqrt{\frac{-\alpha_{11}+\sqrt{\alpha_{11}^2-3\alpha_{11}(\alpha_1-Q_{12}\sigma)}}{3\alpha_{111}}}. \quad (7)$$

In addition, dielectric constant ε_{33} is also derived from the second partial derivative stability condition

$$\frac{\partial^2 \Delta G}{\partial P_3^2}=\frac{1}{\varepsilon_{33}},$$

$$\varepsilon_{33}=\{2\alpha_1+12\alpha_{11}P_3^2+30\alpha_{111}P_3^4-2Q_{12}\sigma\}^{-1}. \quad (8)$$

In the case of epitaxial PZT films with *c*-axis orientation, the electric properties can be determined using four free energy coefficients of α_1, α_{11}, α_{111}, and Q_{12}. However it has been difficult to determine the free energy coefficients since bulk PZT is a polycrystalline structure and the spontaneous polarization P_3 cannot be measured without single crystal

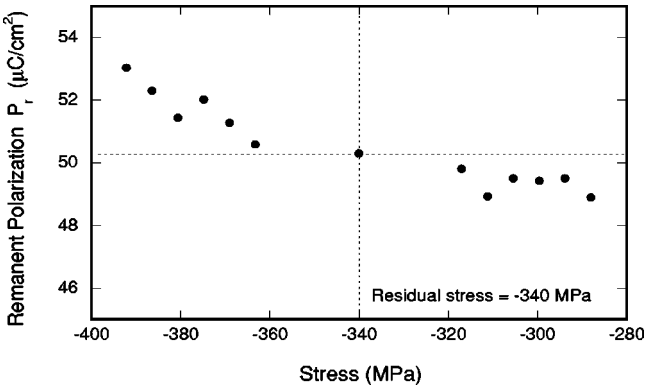

FIG. 6. Remanent polarization of the epitaxial PZT films as a function of the one-dimensional stress.

samples. Haun *et al.* derived these coefficients of PZT by the indirect method from the combination of spontaneous strain and electrostrictive constants. In this study, we prepared single crystalline PZT in a thin film form and could measure the actual spontaneous polarization P_3 which is equal to the remanent polarization because the PZT films were epitaxially grown with the *c*-axis orientation. Therefore we could determine the free energy coefficients directly from the experimental data.

D. Calculation of the dielectric stiffness coefficients α_1, α_{11}, α_{111}, and the electrostrictive coefficient Q_{12}

We determined free energy coefficients from the experimental data of dielectric constant and spontaneous polarization. From Eqs. (7) and (8), the dielectric constant and the spontaneous polarization are expressed as a function of the one-dimensional internal stress along the *a* axis:

$$3\alpha_{111}P_3^4+2\alpha_{11}P_3^2+(\alpha_1-Q_{12}\sigma)=0, \tag{9}$$

$$15\alpha_{111}P_3^4+6\alpha_{11}P_3^2+(\alpha_1-Q_{12}\sigma)=\frac{1}{2\varepsilon_{33}}. \tag{10}$$

We determined free energy coefficients applying stress dependences of dielectric and ferroelectric properties to the above equations. Although the dielectric constants showed clear dependence on the stress, the values of remanent polarization showed significant variation and it is difficult to determine the reliable constant of proportionality. On the other hand, the proportional ratio between polarization and stress (dP_3/dX_1) represents the piezoelectric coefficient d_{31} and we have estimated the stable piezoelectric coefficient d_{31} of -100×10^{-12} m/V for the *c*-axis-oriented epitaxial PZT films with the same composition.[23] Therefore we use the piezoelectric coefficient d_{31} to determine polarization dependence on the stress instead of the experimental results as shown in Fig. 6.

The piezoelectric coefficient d_{31} is expressed using the electrostrictive coefficients Q_{12} as

$$d_{31}=\frac{dP_3}{dX_1}=\frac{\partial^2\Delta G}{\partial X_1\partial P_3}\cdot\frac{\partial^2 P_3}{\partial\Delta G^2}=2\varepsilon_{33}Q_{12}P_3. \tag{11}$$

Using the dielectric constant and spontaneous polarization in the neutral stress, the electrostrictive coefficients Q_{12} can be obtained to be -5.70×10^{-2} (m^4/C^2).

The dielectric stiffness coefficients α_1, α_{11}, α_{111} was determined using the data of dielectric constants at representative stress states of -380, -340, and -260 MPa. Spontaneous polarization at any stress can be obtained by

$$P_3(\sigma)=P_3(-340)+\frac{dP_3(\sigma)}{dX_1}\Delta\sigma$$
$$=P_3(-340)+d_{31}(\sigma+340)\times10^6, \tag{12}$$

where $P_3(\sigma)$ is the spontaneous polarization at the stress of σ MPa. From Eqs. (9) and (10), the dielectric stiffness coefficients α_1, α_{11}, α_{111} should satisfy the equation

TABLE II. Comparison of electric properties and free energy coefficients between bulk PZT and epitaxial PZT film

	bulk PZT (Ref. 5)	epitaxial PZT film
Dielectric constant ε (F/m)	3.38×10^{-9}	1.74×10^{-9}
Spontaneous polarization Ps ($\mu C/cm^2$)	50	50.3
α_1 (m/F)	-4.887×10^7	-1.30×10^8
α_{11} (m^5/C^2 F)	4.764×10^7	3.07×10^8
α_{111} (m^9/C^2 F)	1.336×10^8	-3.11×10^7
Q_{12} (m^4/C^2)	-4.6×10^{-2}	-5.70×10^{-2}

$$\begin{pmatrix}1 & 6P_{\sigma1}^2 & 15P_{\sigma1}^4\\ 1 & 6P_{\sigma2}^2 & 15P_{\sigma2}^4\\ 1 & 2P_{\sigma0}^2 & 3P_{\sigma0}^4\end{pmatrix}\begin{pmatrix}\alpha_1\\ \alpha_{11}\\ \alpha_{111}\end{pmatrix}=\begin{pmatrix}Q_{12}\sigma_1+1/\varepsilon_{\sigma1}\\ Q_{12}\sigma_2+1/\varepsilon_2\\ Q_{12}\sigma_0\end{pmatrix}, \tag{13}$$

where σ_0, σ_1, and σ_2 are -340, -380, and -260 MPa, respectively. The subscripts of σ_0, σ_1, and σ_2 in P and ε represent the stress states of spontaneous polarization P_3 and dielectric constant ε_{33}. The spontaneous polarization and dielectric constant can be determined from Eq. (12) and Fig. 4. Then, the dielectric stiffness coefficients α_1, α_{11}, and α_{111} were calculated to be, $\alpha_1=-1.30\times10^8$ (m/F), $\alpha_{11}=3.07\times10^8$ (m^5/C^2F), $\alpha_{111}=-3.11\times10^7$ (m^9/C^2F).

The comparison of the electric properties and the free energy coefficients between bulk $Pb(Zr_{0.5}Ti_{0.5})O_3$ by Haun *et al.*[5] and epitaxial $Pb(Zr_{0.52}Ti_{0.48})O_3$ films of our experiments were listed in Table II. Although spontaneous polarization and electrostrictive coefficients were almost the same as Haun's results, the dielectric constant and dielectric stiffness coefficients of our results were significantly different. These results suggest that it is necessary to use the data of the PZT films instead of the previous bulk values for the estimation of the thermodynamic characteristics of the epitaxial PZT films.

The electric properties of the PZT films could be estimated as a function of the stress using the values listed in Table II. Figure 7 shows the relationship between relative dielectric constant and one-dimensional stress on the PZT films. The dielectric properties obtained from Haun's data of $Pb(Zr_{0.5}Ti_{0.5})O_3$ are also plotted in Fig. 7. This figure represents that the dielectric constant of the epitaxial films increases with one-dimensional stress, but the increase ratio is significantly smaller than the data from bulk PZT, suggesting that epitaxial PZT films have relatively stable dielectric dependence on stress. On the other hand, Fig. 8 shows spontaneous polarization of the epitaxial PZT films as a function of one-dimensional stress. The spontaneous polarization shows almost same dependence as conventional data and it gradually decreases with stress.

E. Dependence of dielectric constant on temperature

It is known that the dielectric properties of ferroelectric materials strongly depend on temperature in accordance with

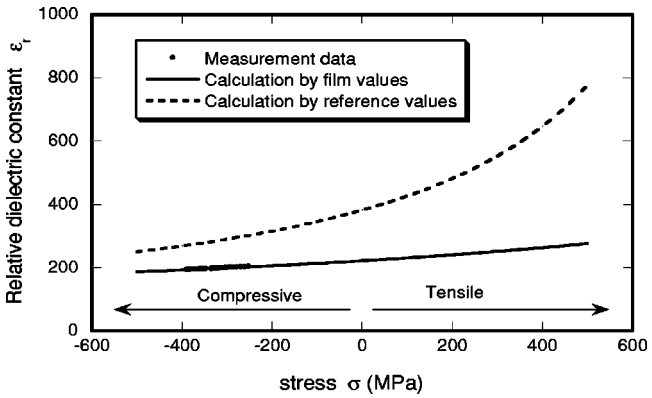

FIG. 7. Dependence of relative dielectric constant on the one-dimensional stress estimated using the free energy coefficients of the bulk and thin film PZT.

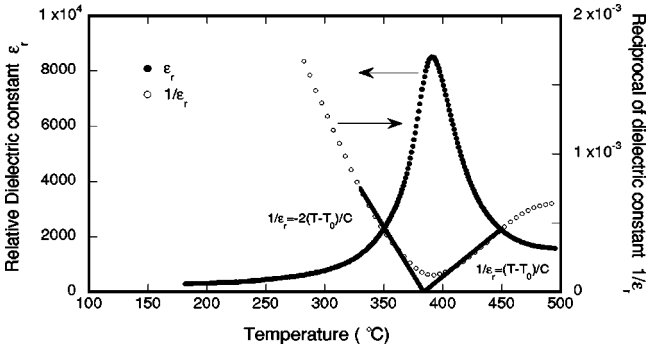

FIG. 9. Temperature dependence of dielectric property. Relative dielectric constants ε_r and reciprocal of relative dielectric constants $1/\varepsilon_r$ were plotted as a function of temperature. Solid lines represent the Curie-Weiss law of $T_0=384$ and $C=1.44\times10^5$ °C.

the Curie-Weiss law. In the dielectric stiffness coefficients, α_1 depends on temperature and can be defined as

$$\alpha_1=(T-T_0)/2\varepsilon_0 C, \tag{14}$$

where C is Curie constant, ε_0 is dielectric constant of free space, and T_0 is the Curie-Weiss temperature. Therefore dielectric constants in paraelectric and ferroelectric phases are expressed as

$$1/\varepsilon_{33}=(T-T_0)/\varepsilon_0 C \quad (T>T_0),$$

$$1/\varepsilon_{33}=-2(T-T_0)/\varepsilon_0 C \quad (T\leqslant T_0). \tag{15}$$

In this experiment, we observed the dielectric constant as a function of temperature, and evaluated the dielectric stiffness coefficient of α_1 in order to confirm the validity of the free energy coefficient obtained by stress dependence. Figure 9 shows the relationship between dielectric constants of the PZT films and temperature. The dielectric constant gradually increased and exhibited the maximum at the ferroelectric-paraelectric phase transition temperature. The reciprocal plot of dielectric constant is good agreement with the Currie-Weiss law as shown in Fig. 9. The Curie-Weiss temperature was determined as 384 °C, which is almost the same as bulk $Pb(Zr_{0.5}Ti_{0.5})O_3$ of 392.6 °C.[5] The Curie constant of epitaxial PZT films was obtained from Fig. 9 as $C=1.44\times10^5$ °C, which was smaller than that of bulk PZT (4.247×10^5 °C). On the other hand, the dielectric stiffness coefficients α_1 at a room temperature is also determined from Eq. (12) as -1.37×10^8 m/F, which is almost the same as the value derived in the previous section (-1.30×10^8 m/F). This result indicates that the dielectric dependence on temperature has proved the validity of dielectric stiffness coefficients of single crystalline and single domain PZT films obtained by the estimation of electric dependence on one-dimensional stress.

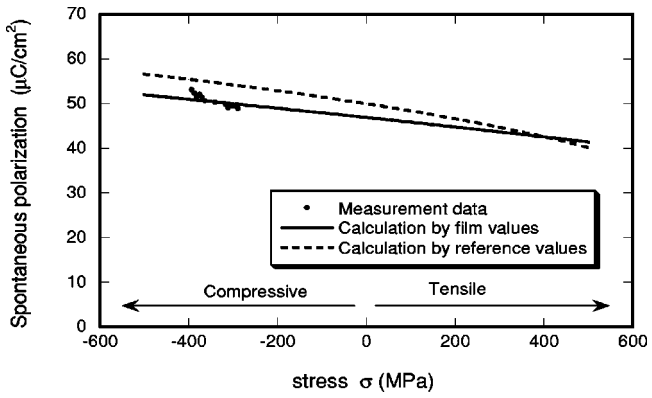

FIG. 8. Dependence of spontaneous polarization on the one-dimensional stress estimated using the free energy coefficients of the bulk and thin film PZT.

IV. CONCLUSIONS

We prepared *c*-axis-oriented epitaxial PZT films with the composition of Zr/Ti=52/48 and investigated thermodynamic characteristics. The dielectric and ferroelectric properties of epitaxial films depend on external stress and their characteristics were examined on the basis of the Landau-Devonshire's phenomenological theory. The dielectric stiffness coefficients and the electrostrictive coefficient of epitaxial PZT films were obtained as $\alpha_1=-1.30\times10^8$ (m/F), $\alpha_{11}=3.07\times10^8$ (m^5/C^2F), $\alpha_{111}=-3.11\times10^7$ (m^9/C^2F), and $Q_{12}=-5.70\times10^{-2}$ (m^4/C^2), which are different than the values derived from the analysis of polycrystalline PZT. The temperature dependence of dielectric constant demonstrated that the dielectric properties obeyed Curie-Weiss law. The dielectric stiffness coefficient of α_1 calculated from the temperature dependence was almost the same as the value obtained from the analysis of the stress dependence of the PZT films.

ACKNOWLEDGMENTS

This study was supported by the Industrial Technology Research Grant Program in 2003 from the New Energy and Industrial Technology Development Organization (NEDO) of Japan.

[1] A. Amin, R. E. Newnham, and L. E. Cross, Phys. Rev. B **34**, 1595 (1986).
[2] T. Yamamoto, Jpn. J. Appl. Phys. **35**, 5104 (1996).
[3] T. Yamamoto, Jpn. J. Appl. Phys. **37**, 6041 (1998).
[4] M. J. Haun, E. Furman, S. J. Jang, H. A. McKinsry, and L. E. Cross, J. Appl. Phys. **62**, 3331 (1987).
[5] M. J. Haun, E. Furman, S. J. Jang, and L. E. Cross, Ferroelectrics **99**, 13 (1989).
[6] M. J. Haun, T. J. Harvin, M. T. Lanagan, Z. Q. Zhuang, S. J. Jang, and L. E. Cross, J. Appl. Phys. **65**, 3173 (1989).
[7] J. F. Scott and C. A. Paz de Arajuo, Science **246**, 1400 (1989).
[8] A. M. Flynn, L. S. Tavrow, S. F. Bart, R. A. Brooks, D. J. Ehrlich, K. R. Udayakumar, and L. E. Cross, J. Microelectromech. Syst. **1**, 44 (1992).
[9] P. Muralt, M. Kohli, T. Maeder, A. Kholkin, K. Brooks, N. Setter, and R. Luthier, Sens. Acta. A **48**, 157 (1995).
[10] S. H. Oh and H. M. Jang, Appl. Phys. Lett. **72**, 1457 (1998).
[11] A. K. Tagantsev, N. A. Pertsev, and A. G. Zembilgotov, J. Korean Phys. Soc. **32**, S1457 (1998).
[12] S. H. Oh and H. M. Jang, J. Appl. Phys. **85**, 2815 (1999).
[13] S. H. Oh and H. M. Jang, Phys. Rev. B **63**, 132101 (2001).
[14] S. H. Oh and H. M. Jang, Phys. Rev. B **62**, 14 757 (2000).
[15] R. Takayama and Y. Tomita, J. Appl. Phys. **65**, 1666 (1989).
[16] K. Iijima, I. Ueda, and K. Kugimiya, Jpn. J. Appl. Phys. **30**, 2149 (1991).
[17] K. Nagashima, M. Aratani, and H. Funakubo, J. Appl. Phys. **89**, 4517 (2001).
[18] I. Kanno, H. Kotera, K. Wasa, T. Matsunaga, T. Kamada, and R. Takayama, J. Appl. Phys. **93**, 4091 (2003).
[19] I. Kanno, H. Kotera, K. Wasa, T. Matsunaga, T. Kamada, and R. Takayama, J. Korean Phys. Soc. **42**, S1317 (2003).
[20] T. Matsunaga, T. Hosokawa, Y. Umetani, R. Takayama, and I. Kanno, Phys. Rev. B **66**, 064102 (2002).
[21] K. S. Lee, J. H. Choi, J. Y. Lee, and S. Baik, J. Appl. Phys. **90**, 4095 (2001).
[22] D. H. Chung, Philos. Mag. **8**, 833 (1963).
[23] I. Kanno, S. Fujii, T. Kamada, and R. Takayama, Appl. Phys. Lett. **70**, 1378 (1997).
[24] S. Aggarwal, S. B. Ogale, C. S. Ganpule, S. R. Shinde, V. A. Novikov, A. P. Monga, M. R. Burr, R. Ramesh, V. Ballarotto, and E. D. Williams, Appl. Phys. Lett. **78**, 1442 (2001).